

Spin-dependent electron-hole capture kinetics in luminescent conjugated polymers

Stoyan Karabunarliev* and Eric R. Bittner†

Department of Chemistry, University of Houston, Houston, TX 77204-5003

(Dated: May 21, 2019)

Electron-hole (e-h) capture in luminescent conjugated polymers (LCPs) is modeled by the dissipative dynamics of a multilevel electronic system coupled to a phonon bath. Focusing entirely upon long PPV chains, we consider the recombination kinetics of an initially separated CT pair and address the issue of electroluminescent enhancement in organic light-emitting diode materials. Our model calculations for various length polymers indicate that the ratio of the singlet to triplet formation ratios, $r = \sigma_S/\sigma_T$, is inversely related to the ratio of the singlet and triplet binding energies, $\varepsilon_S^b/\varepsilon_T^b$.

PACS numbers: 78.60.Fi 73.61.Ph

INTRODUCTION

The efficiency of electroluminescence (EL) from organic semiconductors in light emitting diodes (LEDs) is largely determined by the fraction of injected electron-hole pairs which combine within the device to form emissive singlet excitons as opposed to non-emissive triplet states. If one assumes that the cross-sections for singlet and triplet capture are equivalent, then the singlet population fraction, $\chi_S = \sigma_S/(\sigma_S + 3\sigma_T)$ will be limited to 25% according to spin multiplicity. Nonetheless, efficiencies corresponding to $\chi_S = 50\%$ have been achieved independently on poly-phenylenevinylene (PPV based LEDs [2, 3, 4]. From this it has been inferred that in organic light-emitting polymers, singlet e-h capture is intrinsically more efficient than the respective triplet process ($\sigma_S > \sigma_T$). Moreover, recent PA/PADMR experiments on a wide variety of organic polymer systems indicate that the formation ratio $r = \sigma_S/\sigma_T$ typically lies between 2-5 for conjugated polymer systems[5] and that the ratio varies nearly linearly with conjugation length[6].

The observed variation of r with optical gap[5] was originally interpreted according to an interchain recombination model [7]; however, more recent experiments indicate that large values of r are characteristic of extended intrachain conjugation [6]. Moreover, Wilson, *et al.* have measured χ_S and χ_T consistent with $r \approx 4$ for a polymer but only $r \approx 0.9$ for the monomer. [4] While time-dependent scattering calculations by Kobra and Bittner indicate that the weakly bound S_1 exciton is a more efficient trap of free e-h pairs than the tightly bound and highly localized T_1 triple exciton [8], the systematic linear variation of r with (effective) conjugation length n has remained unclear.

This Letter addresses the spin-dependent formation cross-section of singlet and triplet excitons in linear organic conjugated polymers. To our knowledge, ours is the first molecular based model which accurately reproduces this linear relation for a specific molecular system and provides a rationalization for this trend based upon the variation of the exchange energy and the ratio of the sin-

glet/triplet binding energies with increasing chain length. This has important ramifications in the design and synthesis of polymer materials for device applications.

Our model simulates the dissipative relaxation of a multi-level electronic system coupled to a phonon bath. The Hamiltonian for the extended system is given by

$$\hat{H} = \hat{H}_{el} + \hat{H}_{ph} + \hat{H}_{el-ph}. \quad (1)$$

The electronic part, \hat{H}_{el} is the configuration interaction Hamiltonian for singly excited π -electronic configurations for a generic two-band polymer in a localized basis. [9] The configurations, $|\mathbf{m}\rangle = |\overline{m}m\rangle$ taken over valance and conduction-band Wannier functions $|\overline{m}\rangle$ and $|m\rangle$ represent geminate ($\overline{m} = m$) and charge-transfer ($\overline{m} \neq m$) pairs. H_{el} is parameterized from the π -band structure of extendend PPV. Since the conjugation backbone is alternant, the CI integrals $F_{mn} = \delta_{\overline{m}m}\langle m|f|n\rangle - \delta_{mn}\langle \overline{m}|f|\overline{n}\rangle$ of the band structure operator f obey electron-hole symmetry with $\overline{f}_r = -f_r$. Spin dependency originates from the two-body interactions with $V_{mn} = -\langle m\overline{n}||n\overline{m}\rangle + 2\langle m\overline{n}||\overline{m}n\rangle$ for singlets and $V_{mn} = -\langle m\overline{n}||\overline{n}m\rangle$ for triplets. Assuming zero-differential overlap except for geminate orbitals, we take into account only true Coulomb and exchange terms, $\langle m\overline{m}||m\overline{m}\rangle$ and $\langle \overline{m}\overline{m}||\overline{m}m\rangle$, and (transition) dipole-dipole interactions $\langle m\overline{n}||\overline{m}n\rangle$ between geminate singlet pairs. The electron-phonon coupling term assumes that localized conduction/valence levels, $\pm f_o$ and nearest-neighbor transfer integrals $\pm f_1$ are modulated by the phonons q_μ . The linear coupling between electrons and phonons is adjusted empirically to reproduce the vibronic single photon emission and absorption structure of PPV. Finally, the phonon terms consists of two sets of local oscillators with weak nearest neighbor coupling representing two dispersed optical phonon branches centered at 1600 and 100cm^{-1} respectively. These roughly correspond to the C=C bond stretches and ring torsional modes which dominate the Franck-Condon activity in PPV. [10] In a separate publication we present the computational details of our model and its parameterization. [11]

Diagonalizing H_{el} and H_{ph} at the ground state equi-

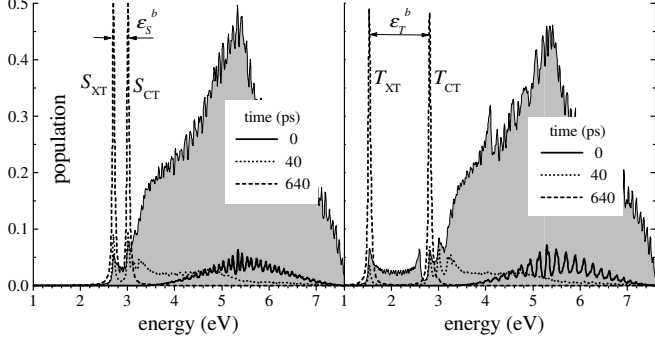


FIG. 1: Density of spin-singlet (left) and spin-triplet (right) states for PPV₃₂ and their populations at different recombination stages. The $t = 0$ population is the initial charge-transfer state projected onto the energy states. Shaded curve is the total density of states for the singlet and triplet manifolds.

librium geometry yields a series of vertical (diabatic) excited states with energies ε_a^o and a normal modes with frequencies ω_ξ . Written in the diabatic representation

$$\begin{aligned} \tilde{H} = & \sum_a \varepsilon_a^o |\mathbf{a}\rangle\langle\mathbf{a}| + \frac{1}{2} \sum_\xi (\omega_\xi^2 Q_\xi^2 + P_\xi^2) \\ & + \sum_{ab\xi} g_{ab\xi}^o Q_\xi |\mathbf{a}\rangle\langle\mathbf{b}|. \end{aligned} \quad (2)$$

The diabatic states, the vibrational normal modes, and diabatic couplings, $g_{ab\xi}^o$, allow us to compute the time-evolution and phononic relaxation of an arbitrary excitonic or charge transfer state. In the absence of e-h symmetry, dipole-dipole coupling between singlet geminate and non-geminate configurations is introduced through this term. As we shall explore later, this opens a channel for coupling singlet charge-transfer states to singlet excitonic states but does not allow for coupling between the triplet CT to XT states.

Separated CT states are not eigenstates of the diabatic Hamiltonian and will evolve in time according to the time-dependent Schrödinger equation. While a complete description of the vibronic dynamics is unfeasible due to the enormous size of the state-space, we can consider the phonons as a dissipative finite-temperature bath for the electrons and derive reduced equations of motion for the electronic dynamics. For this we turn to the Liouville-von Neumann equation for the evolution of the electronic density matrix,

$$i\hbar\dot{\rho} = [\tilde{H}_{el}, \rho] + \frac{i}{\hbar}\mathcal{R}\rho, \quad (3)$$

where the first term represents the unitary evolution of the uncoupled electronic states in the diabatic representation and the second term the non-unitary, dissipative dynamics due to the coupling to the phonon bath. Since the electronic state-space consists 100 to 1000 energy levels depending upon the size of the polymer chain, we

restrict our attention to the population dynamics and decouple populations from coherences according to the Bloch model,

$$\mathcal{R}_{aabb} = -k_{ab} + \delta_{ab} \sum_c k_{ac} \quad (4)$$

$$\mathcal{R}_{abab} = \frac{1}{2} \sum_c (k_{ac} - k_{bc}) \quad (5)$$

where k_{ab} are the rates of elementary interstate transitions. For internal conversions within the diabatic excited states, we assume that the phonons thermalize rapidly on the time-scale of the electronic dynamics such that the one-phonon transitions rates can be determined within the Markov approximation

$$k_{ab} = \pi \sum_\xi \frac{(g_{ab\xi}^o)^2}{\hbar\omega_\xi} (n_\xi + 1) (\Gamma(\omega_\xi - \omega_{ab}) - \Gamma(\omega_\xi + \omega_{ab})) \quad (6)$$

Here n_ξ is the Bose-Einstein distribution of phonons at $T = 300\text{K}$ and Γ is the empirical broadening of 0.01eV . We note that we compute the diabatic coupling terms, $g_{ab\xi}^o$ with respect to the ground-state (S_o) equilibrium geometry so that our approach does not account for any self-localization or dressing in the excited state. Note further that for an elementary $a \rightarrow b$ population transfer to occur there must a phonon mode ω_ξ at that transition frequency ω_{ab} . Thus, phonon mediated dynamics is restricted to the excited state manifold where the energy level spacing is commensurate with the phonon energies. In essence, so long as the non-equilibrium vibrational dynamics is not a decisive factor, we can use these equations to trace the relaxation of an electronic photo- or charge-transfer excitation from its creation to its decay including photon outflow measured as luminescence.

In modeling of e-h capture, propagation starts from the free e-h pair represented by the charge-transfer (CT) configuration with an electron and a hole separated on the far ends of the polymer chain, and the spectral distribution of the starting configuration in S and T state-spaces for a 32 repeat unit chain PPV₃₂. Singlet and triplet populations are also given at an intermediate stage of relaxation at 40ps and at 640ps when the process is practically complete. In both singlet and triplet cases, the system evolves to a metastable state, where half of the density remains locked in CT states (S_{CT} or T_{CT}) while the other half decays fully into the lowest excitonic states (S_{XT} or T_{XT}). The branching into CT and XT channels is due to e-h symmetry, which separates excited states into even and odd representations under e-h transposition. Thus, XT states, which are even, are not vibronically coupled to CT states, which are odd. As shown in Fig.2a, S_{XT} and T_{XT} are formed at different rates. Whereas S_{XT} , S_{CT} and T_{CT} show almost parallel population growths, formation of T_{XT} is far slower.

Assuming that after an initial approach time, the formation of the lowest energy excitons follows first-order

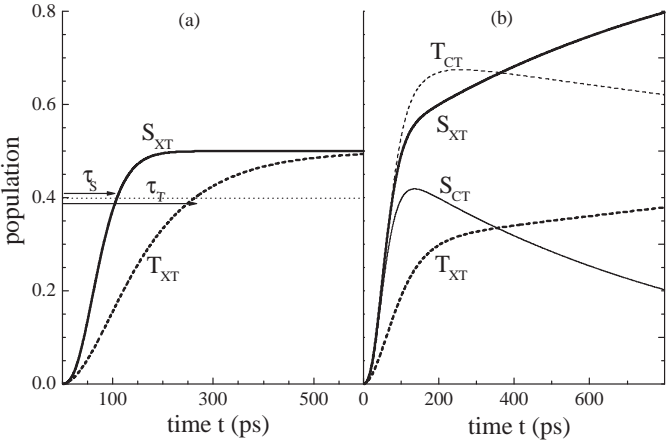


FIG. 2: Essential-state populations as a function of time for PPV₃₂ with strict (a) and weakly broken (b) e-h symmetry. The S_{CT} and T_{CT} populations not shown in (a) follow closely the S_{XT} curve.

kinetics corresponding to the decay of some precursor state. While population buildup clearly deviates from first-order kinetics at the earliest stages, we can measure the relative efficiency of exciton formation by the time τ at which the exciton population reaches 40% and relate the formation cross-section and formation times by $\tau \propto 1/\sigma$. These values are plotted in Fig. 3a vs. inverse conjugation length $1/n$. The absolute formation time for the singlet reaches an asymptotic limit at about 10-16 repeat units where as the formation times for the triplet continue to increase almost exponentially. For the longest chain considered (PPV₃₂), the formation times are $\tau(S_{XT}) = 108$ ps and $\tau(T_{XT}) = 262$ ps, the cross-section ratio, $r = \tau_T/\tau_S = 2.5$, and a EL efficiency of 45.5% which is in good agreement with both EL[1, 2, 3] and the PA/PADMR data. [5, 6] Moreover on the short end of the scale, the computed behaviour is consistent with experimental data for very short oligomers and monomers in which triplet formation is more effective. [4]

Using the density of states we compute for each chain, we can define the binding energy, ε^b , for the singlet and triplet states as the energy difference between the lowest lying excitonic bound state, ε_{XT} and the bottom of the continuum of unbound states lying above the highest lying excitonic state, ε_{CT} . For this we identify the lowest unbound state as the lowest lying odd-symmetry state (i.e. a charge-transfer state) for both the singlet and triplet species. In Fig. 1 these can be identified by the position of the two peaks representing the time-evolved population densities. These we plot in Fig. 3a and note convergence of both ε_S^b and ε_T^b with increasing n , corresponding to an effective conjugation length of ≈ 10 repeat units.

In general, the binding energies for both the singlet

and triplet decrease with increasing chain length as seen in Fig. 3a. However, the difference between the singlet and triplet binding energies remains almost constant at roughly 1 eV for all chain lengths reflecting the parametrization of the exchange interaction between geminate electron-hole pairs. As seen for the longest chain considered in Fig. 1, the singlet excitonic band S_{XT} nearly overlaps with the charge-transfer band S_{CT} , whereas in the case of the triplet exciton, T_1 lies at the bottom of a separate band of bound e-h pairs, 1.32eV below the CT continuum. Thus T_{XT} formation requires on average a longer sequence of vibron-mediated transitions, each falling into the phonon frequency range. On the other hand, the singlet binding energy ranges from 1.3eV (for $n = 2$) to 0.3 eV (for $n = 32$) requiring the excitation of significantly fewer phonons to relax from the lowest unbound singlet to the lowest bound singlet.

In Fig. 3b we plot r vs $1/n$ and establish an excellent agreement with experiments [5, 6] for both long and short oligomers including a notable triplet enhancement ($r < 1$) for $n < 3$ [4]. This indicates that LED device performance will generally improve if one chooses materials with longer conjugation lengths. One speculative explanation is that the singlet is generally delocalized over the entire conjugation length while the triplet is more tightly bound and more localized. Consequently, increasing n will accentuate the differences between these two states which should be reflected in the excitonic binding energies. Plotting the ratio of the binding energies $\varepsilon_T^b/\varepsilon_S^b$ vs. $1/n$, we obtain a remarkable correlation between $\varepsilon_T^b/\varepsilon_S^b$ and r .

If we write the branching ratio $r(n)$ in terms of the ratio of transition matrix elements from some precursive

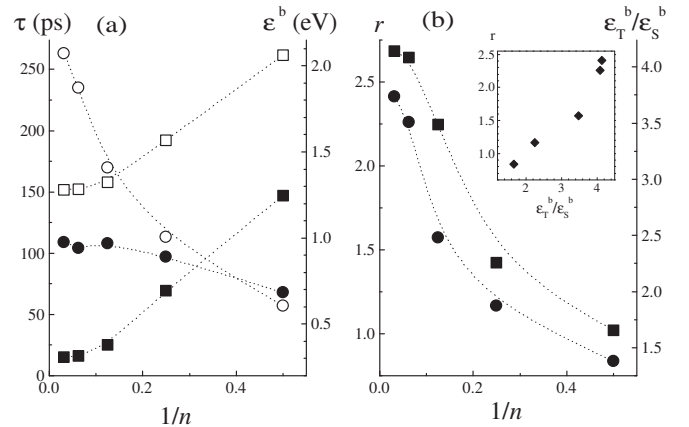


FIG. 3: (A) Variation of singlet and triplet binding energies and formation times with inverse conjugation length. ($\tau_T = \circ$, $\tau_S = \bullet$, $\varepsilon_T^b = \square$, $\varepsilon_S^b = \blacksquare$). (B) Binding energy $\varepsilon_T^b/\varepsilon_S^b$ (\bullet) and formation-time ratio τ_T/τ_S (\blacksquare) vs. inverse inverse conjugation length. Inset: $\varepsilon_S^b/\varepsilon_T^b$ vs. r for various conjugation lengths. Dashed curves are simply spline fits meant to guide the eye.

unbound state to the lowest exciton state, then we can approximate

$$r(n) = \frac{\tau_T}{\tau_S} \propto r_{vib} \frac{\varepsilon_T^b}{\varepsilon_S^b} \quad (7)$$

where r_{vib} is the ratio of effective multi-phonon vibronic matrix elements coupling the two states. If r_{vib} prefactor varies only weakly in n , then we can approximate $r(n) \approx \varepsilon_T^b / \varepsilon_S^b$. In the inset of Fig. 3b we plot $r(n)$ vs. $\varepsilon_T^b / \varepsilon_S^b$ and obtain nearly linear correlation between the two computed quantities. This confirms our assumption that the matrix elements coupling the lowest unbound electron-hole state to the lowest bound electron-hole state has the same parametric dependency in n for both singlet and triplet cases.

Thus, the intrinsic distinction between S and T e-h captures is readily understood almost entirely in terms of the exciton binding energies, which is in itself a direct measure of the relative exchange interaction. The exchange interaction term destabilizes geminate e-h pairs for singlets. Consequently, singlet XT states have proportionally fewer geminate configurations than their triplet counterparts for which exchange provides a stabilizing effect. Apart from spin-degeneracy statistics, efficiency of singlet e-h capture outweighs the triplet one as a natural outcome of the higher binding energy of triplet excitons. For both S and T processes, the relaxation mechanism involves two steps as a result of approximate e-h symmetry. In the initial e-h capture, both low-lying excitons and same-spin CT intermediates are formed. The XT to CT branching ratio may vary, but is inevitably more favorable for singlet excitons than for triplet ones simply due to energetics. Relaxing to the higher lying singlet exciton requires fewer elementary relaxation steps than the lower lying triplet exciton.

The higher efficiency of S recombination becomes more apparent when e-h symmetry is lifted. We slightly broaden the conduction band and squeeze the valence band, so that $f/\bar{f} = -1.1$. The small e-h asymmetry changes negligibly the electronic spectrum, but opens a weak vibronic channel for CT \rightarrow XT internal conversions. The resulting population dynamics are shown in Fig. 2b. Here we see a fast build-up of low-lying XT and CT states in the first 100 to 200ps, followed by a slow conversion of CT states into excitons. The initial dynamics occurs approximately without e-h parity crossovers and the formation rates of low-lying XT and CT singlets and triplets are about the same as in the symmetric case. However, the triplet XT to CT branching ratio decreases drastically to about 1:2 and suppresses the formation of T_{XT} . Moreover, subsequent $T_{CT} \rightarrow T_{XT}$ relaxation is very slow due to the large binding energy of triplet excitons and the low density of states between T_{CT} and T_{XT} . In contrast, S_{XT} is slightly favored over S_{CT} in the initial capture, and further $S_{CT} \rightarrow S_{XT}$ conversion occurs on a time scale of about 800ps. The weak e-h asymmetry of real

conjugated systems favors again the singlet $CT \rightarrow XT$ relaxation by a factor, commensurate with the ratio of T to S exciton binding energies. Note as well that S_{CT} and T_{CT} are very close in energy because of the lack of appreciable exchange between separated electrons and holes. Hence, intersystem $S \rightarrow T$ crossing of long-lived CT states due to spin-orbit coupling is highly likely to occur prior to final e-h binding.

In summary, we have simulated phonon-mediated intrachain e-h recombination in LCPs. The approach allows us to examine EL quantum yield in LCPs further case by case by combining a first-principle description with available spectroscopic data. The results for our calculations are consistent with the spin-resolved experiments in all essential points. While we focus here on PPV, our results can be generalized to most nondegenerate polymers. Recombination is an intrachain relaxation process in the excited state-space. The efficiency and hence the rate of relaxation is inversely proportional to the amount of energy which must be dissipated to the lattice vibrations. Hence while strong on-site vibronic coupling is responsible for $r < 1$ for the short chains and molecular species, the disproportion of exciton binding energies accounts for the larger r values in extended polymeric systems. The approximate e-h symmetry of conjugated polymers implies the parallel formation of long-lived charge-transfer pairs, which are nearly spin-independent, and thus susceptible to secondary singlet-triplet relaxation branching or spin-orbit coupling.

This work was funded by the National Science Foundation (CAREER Award) and the Robert A. Welch Foundation.

* email:karabuna@uh.edu

† email:bittner@uh.edu

- [1] J. H. Burroughes et al., *Nature* **347**, 539 (1990).
- [2] Y. Cao et al., *Nature* **397**, 414 (1999).
- [3] R. H. Friend et al., *Nature* **397**, 121 (1999).
- [4] J. S. Wilson, A. S. Dhoot, and A. J. A. B. Seeley, M. S. Khan, A. Köhler, and R. H. Friend, *Nature* **413**, 828 (2001).
- [5] M. Wohlgemann, K. Tandon, S. Mazumdar, S. Ramasesha, and Z. V. Vardeny, *Nature* **409**, 494 (2001).
- [6] M. Wohlgemann, X. M. Jiang, Z. V. Vardeny, and R. A. J. Janssen, *Phys. Rev. Lett.* **88**, 197401 (2002)
- [7] Z. Shuai, D. Beljonne, R. J. Silbey, and J. L. Bredas, *Phys. Rev. Lett.* **84**, 131 (2000); A. Ye, Z. Shuai, and J. L. Bredas, *Phys. Rev. B* **65**, 5208 (2002).
- [8] M. Kobra and E. R. Bittner, *Phys. Rev. B* **62**, 11473 (2000).
- [9] D. Mukhopadhyay, G. W. Hayden, and Z. G. Soos, *Phys. Rev. B* **51**, 9476 (1995); M. Chandross, Y. Shimo, and S. Mazumdar, *Phys. Rev. B* **59**, 4822 (1999).
- [10] S. Karabunarliev, E. R. Bittner and M. Baumgarten, *J. Chem. Phys.* **114**, 5863 (2001).
- [11] S. Karabunarliev and E. R. Bittner, cond-mat/0206015.